Phytochemistry 151 (2018) 119–127

Contents lists available at ScienceDirect

Phytochemistry

journal homepage: www.elsevier.com/locate/phytochem

Pentacyclic triterpenoids from *Cyclocarya paliurus* and their antioxidant activities in FFA-induced HepG2 steatosis cells

Hui-Min Yang [a, b, c, 1], Zhi-Qi Yin [b, 1], Meng-Ge Zhao [b, c], Cui-Hua Jiang [c], Jian Zhang [c, *], Ke Pan [a, **]

[a] Department of Natural Medicinal Chemistry, School of Traditional Chinese Medicine, China Pharmaceutical University, Nanjing 210009, PR China
[b] Department of TCMs Pharmaceuticals, School of Traditional Chinese Medicine, China Pharmaceutical University, Nanjing 210009, PR China
[c] Laboratory of Translational Medicine, Jiangsu Province Academy of Traditional Chinese Medicine, Nanjing 210028, PR China

ARTICLE INFO

Article history:
Received 29 December 2017
Received in revised form
27 March 2018
Accepted 30 March 2018

Keywords:
Cyclocarya paliurus
Juglandaceae
Pentacyclic triterpenoids
Antioxidant effects
FFA-induced hepatic steatosis

ABSTRACT

Six undescribed pentacyclic triterpenoids including four triterpenoid aglycones, 1β,2α,3β,23-tetrahydroxyurs-12-en-28-ursolic acid, 2α,3α,6β,19α,23-pentahydroxyurs-12-en-28-ursolic acid, 2α,3α,20β,23-tetrahydroxyurs-12-en-28-ursolic acid and 1β,2α,3β,23-tetrahydroxyurs-12,20(30)-dien-28-ursolic acid, and two triterpenoid glucosides, 2α,3α,23-trihydroxy-12,20(30)-dien-28-ursolic acid 28-*O*-β-D-glucopyranoside and 1-oxo-3β,23-dihydroxyolean-12-en-28-oic acid 28-*O*-β-D-xylopyranoside, along with 5 known triterpenoids were isolated from a CH_3Cl-soluble extract of the leaves of *Cyclocarya paliurus*. Their structures were established on the basis of chemical and spectroscopic approaches. These compounds were assessed for their antioxidant effects on FFA-induced hepatic steatosis in HepG2 cells. The results revealed that three saponins and two aglycones markedly increased SOD activity and reduced MDA level.

1. Introduction

Cyclocarya paliurus (Batalin) Iljinskaja (Juglandaceae) is a tall tree belonging to the Juglandaceae family and is an endemic species distributed in south and southeast of China (Wu et al., 2014). The leaves of *C. paliurus* have been used by indigenous people for the prevention and treatment of hypertension, dyslipidemia and diabetes (Jiang et al., 2015a; Kurihara et al., 2003). Over the last several decades, phytochemical studies of *C. paliurus* led to the identification of nearly 100 compounds, containing polysaccharides, flavonoids, phenolic acids and triterpenoids (Wu et al., 2017; Xie and Xie, 2008). Various triterpenoid aglycones and glycosides have been identified from the leaves of *C. paliurus*, including pentacyclic and tetracyclic type such as oleanane-, ursane- and dammarane-type triterpenoids (Fu and Fang, 2009; Wang et al., 2016). Previous studies also reported that ethanol extract of *C. paliurus* exhibited antioxidant effects, remarkably lowered the levels of malondialdehyde, and elevated superoxide dismutase activity in type 2 diabetic rats and high-fat diet mice (Ma et al., 2015; Wang et al., 2013). Our findings have demonstrated that ethanol extract of *C. paliurus* leaves was abundant in triterpenic acids and could ameliorate high fat diet-induced hepatic oxidative stress and inflammation, leading to block the development of nonalcoholic fatty liver disease (NAFLD) (Lin et al., 2016). These results indicated that triterpenoids might be the major functional components of *C. paliurus*.

Currently NAFLD has become the most common liver disease with about 20–30% of general population worldwide (Yopp and Choti, 2015). NAFLD includes a series of hepatic pathology ranging from hepatic steatosis to nonalcoholic steatohepatitis, which may trigger the development of fibrosis and cirrhosis, eventually lead to hepatocarcinoma (Choi and Diehl, 2008). Though the precise mechanism of NAFLD is still unknown, its pathogenesis is often described as a "two-hits hypothesis" involving insulin resistance and oxidative stress (Day and James, 1998). Oxidative stress has also been verified to play an important role in the

* Corresponding author. Laboratory of Translational Medicine, Jiangsu Province Academy of Traditional Chinese Medicine, No.100, Shizi Street, Hongshan Road, Qixia District, Nanjing, 210028 Jiangsu Province, PR China.
** Corresponding author. Department of Natural Medicinal Chemistry, School of Traditional Chinese Medicine, China Pharmaceutical University, No.639, Longmian Road, Nanjing, 211198 Jiangsu Province, PR China.
E-mail addresses: zhangjian@jsatcm.com (J. Zhang), pan.ke.nj@gmail.com (K. Pan).
[1] These authors contributed equally.

https://doi.org/10.1016/j.phytochem.2018.03.010
0031-9422/

pathogenesis of NAFLD in animal and human studies (De Almeida et al., 2010; Madan et al., 2006). Furthermore, both malondialdehyde (MDA) and superoxide dismutase (SOD) are important indices of oxidative stress. As a cytotoxic product of lipid peroxidation, MDA impairs nucleotide and protein synthesis, plays a vital role in hepatic fibrogenesis (Leonarduzzi et al., 1997). SOD, an enzyme that catalyzes the dismutation of superoxide radicals into hydrogen peroxide, prevents lipid peroxidation (Jiang et al., 2015b).

In a continuing search for the biological active compounds from *C. paliurus*, six undescribed pentacyclic triterpenes (**1**–**6**) and five known triterpenoids (**7**–**11**) were isolated. These compounds were assessed for their antioxidant effects on FFA-induced hepatic steatosis in HepG2 cells to validate whether they could block the development of NAFLD via ameliorating hepatic oxidative stress.

2. Results and discussion

Compound **1** was obtained as white and amorphous powder. The molecular formula was determined to be $C_{30}H_{48}O_6$ on the basis of HRESIMS (*m/z* 527.3338 $[M+Na]^+$, calcd for $C_{30}H_{48}NaO_6$, 527.3343) and ^{13}C NMR data. In the ^1H NMR spectrum (Table 1), four methyl singlets at δ_H 1.11, 1.20, 1.22, 1.37 (each 3H, s), two methyl doublets at δ_H 0.94 (3H, d, $J = 6.0$ Hz) and 0.99 (3H, d, $J = 6.0$ Hz), an oxygen-bearing methylene group at δ_H 4.23 (1H, d, $J = 12.0$ Hz) and 3.74 (1H, d, $J = 12.0$ Hz), and three oxygenated methine groups at δ_H 4.32 (1H, d, $J = 9.0$ Hz), 4.16 (1H, dd, $J = 9.0$, 9.0 Hz) and 3.71 (1H, d, $J = 9.0$ Hz) were observed. Further, one olefinic proton signal at δ_H 5.61 (1H, br s) was apparent. The ^{13}C NMR spectrum of **1** (Table 1) displayed 30 carbon resonances including a carbonyl carbon (δ_C 180.0), two olefinic carbons (δ_C 138.3 and 127.2), and four oxygenated carbons (δ_C 66.3, 74.4, 74.8, 84.7). Therefore, **1** was assigned as an ursane-type triterpenoid (Singab et al., 2000). The spectroscopic data above were similar to those of a known compound, 1β,2*a*,3β,19α,23-pentahydroxyurs-12-en-28-ursolic acid (Singab et al., 2000) except for the resonances corresponding to a methyl doublet [H-29 (δ_H 0.94, d, $J = 6.0$ Hz); δ_C 39.5 (C-19)] in **1** instead of signals for the H-29 (δ_H 1.44, 3H, s) and C-19 (δ_C 72.5) groups. The 2D structure of **1** was established via thorough analysis of the COSY, HSQC, and HMBC NMR spectra (Fig. 2). The α-orientation of 2-OH was confirmed by the strong NOESY correlation from H-2 to H-25 and H-24 (Fig. 2).The β-orientations of 1-OH and 3-OH were confirmed by the NOESY correlations from H-1 to H-9 and H-3 to H-5, respectively (Fig. 2). Thus, the structure of **1** (Fig. 1) was elucidated as 1β, 2*a*, 3β, 23-

Table 1
^1H [ppm, mult. (*J* in Hz)] and ^{13}C NMR data of compounds **1**–**3** (in C_5D_5N).

Position	1		2		3	
	δ_C[a]	δ_H[b]	δ_C[c]	δ_H[d]	δ_C[c]	δ_H[d]
1	84.7, CH	3.71, d (9.0)	45.4, CH_2	1.98, m	48.3, CH_2	2.28, m
				1.88, m		1.37, m
2	74.4, CH	4.16,dd (9.0,9.0)	66.7, CH	4.45, m	69.3, CH	4.24,ddd (10.5,9.5,4.0)
3	74.8, CH	4.32,d (9.0)	81.1, CH	4.15,d (4.5)	78.8, CH	4.19,d (9.5)
4	43.5, C	–	42.9, C	–	44.0, C	–
5	45.6, CH	1.84, m	44.5, CH	2.30, m	48.4, CH	1.77, m
6	18.1, CH_2	1.83, m	68.4, CH	4.97, m	18.9, CH_2	1.71, m
		1.61, m				1.43, m
7	33.5, CH_2	1.74, m	41.7 CH_2	2.14, m	33.6, CH_2	1.67, m
		1.40, m		1.89, m		1.32, m
8	40.7, C	–	40.3, C	–	40.4, C	–
9	49.1, CH	2.18, m	48.6, CH	2.30, m	48.5, CH	1.84, m
10	43.4, C	–	38.4, C	–	38.7, C	–
11	27.6, CH_2	3.26, m	24.5 CH_2	2.30, m	24.2 CH_2	2.04, m
		2.49, m				
12	127.2, CH	5.61, br s	128.6, CH	5.66, br s	125.8, CH	5.54, br s
13	138.3, C	–	139.7, C	–	139.1, C	–
14	42.6, C	–	43.0, C	–	43.0, C	–
15	28.8, CH_2	2.30, m	29.5, CH_2	2.45, m	29.0, CH_2	2.29, m
		1.20, m		1.27, m		1.13, m
16	25.0, CH_2	2.07, m	26.8, CH_2	3.07, m	25.2, CH_2	2.28, m
		1.96, m		1.99, m		1.97, m
17	48.1, C	–	48.6, C	–	48.2, C	–
18	53.5, CH	2.64,d (12.0)	55.0, CH	3.07, m	51.5, CH	2.89,d (10.0)
19	39.5, CH	1.43, m	73.1, C	–	43.2, CH	2.24, m
20	39.4, CH	0.95, m	42.7, CH	1.50, m	72.7, C	–
21	31.1, CH_2	1.45, m	27.3, CH_2	2.06, m	38.7, CH_2	2.15, m
		1.43, m		1.33, m		1.88, m
22	37.5, CH_2	1.97, m	38.8, CH_2	2.06, m	35.5, CH_2	2.10, m
		1.95, m				1.96, m
23	66.3, CH_2	4.23,d (12.0)	72.2, CH_2	4.16,d (10.0)	67.1, CH_2	4.18,d (10.0)
		3.74,d (12.0)		3.92,d (10.0)		3.72,d (10.0)
24	14.4, CH_3	1.11, s	20.0, CH_3	1.50, s	14.7, CH_3	1.06, s
25	14.0, CH_3	1.37, s	18.9, CH_3	1.72, s	17.9, CH_3	1.07, s
26	18.1, CH_3	1.20, s	18.7, CH_3	1.68, s	18.0, CH_3	1.07, s
27	23.9, CH_3	1.22, s	25.1, CH_3	1.68, s	23.9, CH_3	1.14 s
28	180.0, C	–	181.1, C	–	180.2, C	–
29	21.4, CH_3	0.94,d (6.0)	27.4, CH_3	1.44, s	14.0, CH_3	1.22,d (5.0)
30	17.5, CH_3	0.99,d (6.0)	17.1, CH_3	1.11,d (5.0)	20.4, CH_3	1.38, s

[a] Measured at 75 MHz.
[b] Measured at 300 MHz.
[c] Measured at 125 MHz.
[d] Measured at 500 MHz.

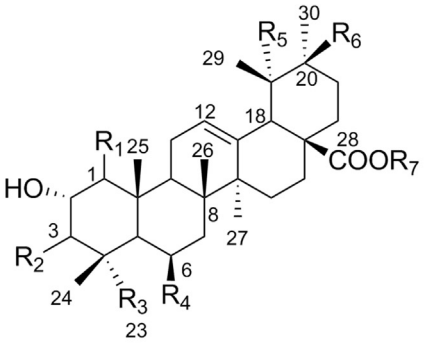

	R_1	R_2	R_3	R_4	R_5	R_6	R_7
1	β-OH	β-OH	CH_2OH	H	H	H	H
2	H	α-OH	CH_2OH	OH	OH	H	H
3	H	α-OH	CH_2OH	H	H	OH	H
7	H	α-OH	CH_2OH	H	H	H	β-D-Glc
8	H	β-OH	CH_2OH	H	OH	H	H
9	H	β-OH	CH_3	H	H	H	H

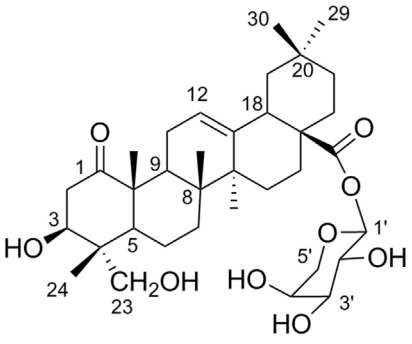

6

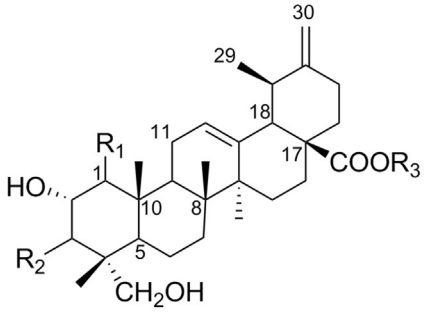

	R_1	R_2	R_3
4	β-OH	β-OH	H
5	H	α-OH	β-D-Glc
10	H	α-OH	H
11	H	β-OH	H

Fig. 1. Chemical structures of compounds **1**–**11**.

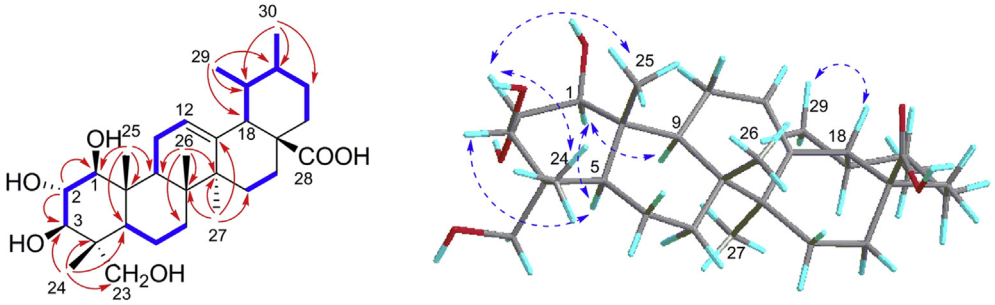

Fig. 2. Key $^1H-^1H$ COSY (—), HMBC (⌒), and NOE (⋯) correlations of **1**.

tetrahydroxyurs-12-en-28-ursolic acid.

Compound **2** was isolated as white and amorphous powder. The molecular formula $C_{30}H_{48}O_7$ was deduced from HRESIMS (*m/z* 538.3738 $[M + NH_4]^+$, calcd for $C_{30}H_{52}NO_7$, 538.3738) and ^{13}C NMR data. The ^1H NMR spectrum of **2** exhibited the typical spectroscopic features of an ursane-type triterpene, including an olefinic proton at δ_H 5.66 (1H, br s), three oxygenated methine protons at δ_H 4.97 (1H, m), 4.45 (1H, m) and 4.15 (1H, d, $J = 4.5$ Hz), a pairs of oxygenated methylene protons at δ_H 4.16 (1H, d, $J = 10.0$ Hz) and 3.92 (1H, d, $J = 10.0$ Hz), five methyl singlets at δ_H 1.44, 1.50, 1.68, 1.68, 1.72 and a methyl doublet at δ_H 1.11 (3H, d, $J = 5.0$ Hz) (Table 1). In addition, the ^{13}C NMR spectrum displayed one carboxylic carbon at δ_C 181.1, five oxygenated carbons at δ_C 66.7, 68.4, 72.2, 73.1, 81.1 as well as two olefinic carbons at δ_C 128.6 and 139.7 (Table 1). These NMR data (Table 1) were almost identical to those of 2α, 3*a*, 19α, 23-tetrahydroxy-12-en-28-ursolic acid (Lee et al., 2005) except for the replacement of one methylene by an additional oxymethine [δ_H 4.97 (1H, m); δ_C 68.4] in **2**. The ^1H–^1H COSY correlations of the oxymethine proton between H-5 and H-7 (Fig. 3) revealed the attachment of an OH group to C-6 in **2**. The NOE interaction of H-5 with H-6 (Fig. 3) confirmed the β-orientation of 6-OH. Therefore, compound **2** (Fig. 1) was elucidated as 2*a*,3*a*,6β,19α,23-pentahydroxyurs-12-en-28-ursolic acid.

Compound **3** appears as white and amorphous powder. Its molecular formula was established as $C_{30}H_{48}O_6$ by HRESIMS (*m/z* 522.3786 $[M + NH_4]^+$, calcd for $C_{30}H_{52}NO_6$, 522.3789) and ^{13}C NMR data. The ^1H NMR spectrum (Table 1) displayed resonances for five methyl singlets (δ_H 1.06, 1.07, 1.07, 1.14, 1.38), a methyl doublet [δ_H 1.22 (3H, d, $J = 5.0$ Hz)], two oxymethines [δ_H 4.24 (1H, ddd, $J = 10.5, 9.5, 4.0$ Hz), 4.19 (1H, d, $J = 9.5$ Hz)], an oxygenated methylene group [δ_H 4.18 (1H, d, $J = 10.0$ Hz), 3.72 (1H, d, $J = 10.0$ Hz)] and an olefinic proton [δ_H 5.54 (1H, br s)]. The ^{13}C NMR spectrum (Table 1) showed 30 carbon resonances comprising four oxygen-bearing carbons (δ_C 67.1, 69.3, 72.7, 78.8), two olefinic carbons (δ_C 139.1 and 125.8) and a carboxylic carbon (δ_C 180.2). These spectrometric data (Table 1) were comparable to those of 2*a*, 3*a*, 23-trihydroxyurs-12-en-28-oic acid (Lee et al., 2008) except for replacement of one methine by an additional oxygenated quaternary carbon (δ_C 72.7) in **3**. Furthermore, the OH group was located at C-20 based on the HMBC cross-peak from H-29 [δ_H 1.22 (3H, d, $J = 5.0$ Hz)] and H-30 [δ_H 1.38 (3H, s)] to C-20 (δ_C 72.7) (Fig. 4). The β-orientation of 20-OH was confirmed by the strong ROESY correlations from H-19 [δ_H 2.24 (1H, m)] to H-30 [δ_H 1.38 (3H, s)]. The configurations of the remaining stereogenic centers were identical to those of 2*a*, 3*a*, 23-trihydroxyurs-12-en-28-oic acid based on the ROESY correlations of **3** (Fig. 4). Accordingly, the structure of **3** (Fig. 1) was defined as 2α, 3α, 20β, 23-tetrahydroxyurs-12-en-28-ursolic acid.

Compound **4** was purified as white and amorphous powder. It showed a molecular formula of $C_{30}H_{46}O_6$ on the basis of the HRESIMS (*m/z* 520.3629 $[M + NH_4]^+$, calcd for $C_{30}H_{50}NO_6$, 520.3633) and ^{13}C NMR data. The ^1H and ^{13}C NMR spectra (Table 2) were almost identical to those of **1** except for the replacement of a methyl signal [δ_H 0.99 (3H, d, $J = 6.0$ Hz)] by the NMR signals due to an exomethylene [δ_H 4.76 (1H, br s), 4.81 (1H, br s); δ_C 154.3, 105.4] in **4**. The location of terminal double bond was deduced at C-20 and C-30 from the HMBC correlations of δ_H 4.76 and 4.81 with C-19 (δ_C 38.1)/C-21 (δ_C 33.2), H-29 (δ_H 1.11) with C-19 (δ_C 38.1)/C-18 (δ_C 56.1)/C-20 (δ_C 154.3) (Fig. 5). The relative configuration of **4** was consistent with that of **1** and confirmed by the NOE interactions in the NOESY spectrum (Fig. 5). Hence, the structure of **4** (Fig. 1) was elucidated as 1β, 2*a*, 3β, 23-tetrahydroxyurs-12,20(30)-dien-28-ursolic acid.

Compound **5** was obtained as white and amorphous powder. It gave the molecular formula $C_{36}H_{56}O_{10}$, according to its HRESIMS at *m/z* 666.4210 $[M + NH_4]^+$ (calcd for 666.4212) and ^{13}C NMR data. The ^{13}C NMR spectrum of **5** showed 36 carbon signals due to the aglycone and one sugar moiety (Table 2). The five sp^3 carbons (δ_C 16.8, 17.6, 18.1, 18.1, 24.0), two sp^2 carbons (δ_C 126.8, 138.6) and a carboxylic carbon (δ_C 176.0) were coupled with the ^1H NMR data which were assigned as four methyl proton singlets (δ_H 1.17, 1.09, 1.05, 0.87), a methyl proton doublet (δ_H 1.04), a broad triplet-like vinyl proton signal (δ_H 5.44). These data indicated that **5** possessed an urs-12-en-28-oic acid skeleton. Furthermore, the ^1H and ^{13}C NMR spectrum (Table 2) exhibited an exomethylene signal [δ_H 4.71, 4.73 (each 1H, br s); δ_C 153.6, 105.6]. The comparison of NMR data (Table 2) with those of 2α,3α,23-trihydroxy-12,20(30)-dien-28-ursolic acid (Sashida et al., 1992) indicated the presence of a β-glucopyranosyl moiety on the basis of the ^{13}C NMR data as well as the coupling constant of the anomeric proton ($J_{H\text{-}1'} = 8.5$ Hz) (Yang et al., 2012). Acid hydrolysis of **5** afforded a D-glucose from HPLC analysis compared with an authentic sugar sample. The linkage of the glucose was verified at C-28 by the HMBC correlation from H-1' (δ_H 6.25) to δ_C 176.0 (Fig. 6). The relative configuration of the aglycone was determined to be 2α, 3α, 23-trihydroxy-12, 20(30)-dien-28-ursolic acid by NOESY spectrum interpretation (Fig. 6). Consequently, compound **5** was assigned as 2*a*, 3*a*, 23-trihydroxy-12, 20(30)-dien-28-ursolic acid 28-*O*-β-D-glucopyranoside (Fig. 1).

Compound **6** was isolated as a white and amorphous powder. Its molecular formula of $C_{35}H_{54}O_9$ was determined from HRESIMS (*m/z* 641.3653 $[M+Na]^+$, calcd for $C_{35}H_{54}NaO_9$, 641.3660) and ^{13}C NMR data. In the ^1H NMR spectrum (Table 2), six methyl singlets (δ_H 1.40, 1.21, 1.19, 1.19, 0.93, 0.89), one olefinic proton signal at δ_H 5.50 (1H, br s), together with one anomeric proton signal at δ_H 6.24 (1H, d, $J = 7.0$ Hz) were observed. The ^{13}C NMR spectrum (Table 2) showed signals at δ_C 213.5, 177.0 (for a keto carbonyl group and an ester carbonyl group), two olefinic carbons signals (δ_C 143.8, 123.7), and an anomeric carbon signal (δ_C 96.7). The analysis of NMR data and comparison with the reference revealed that **6** shared the same

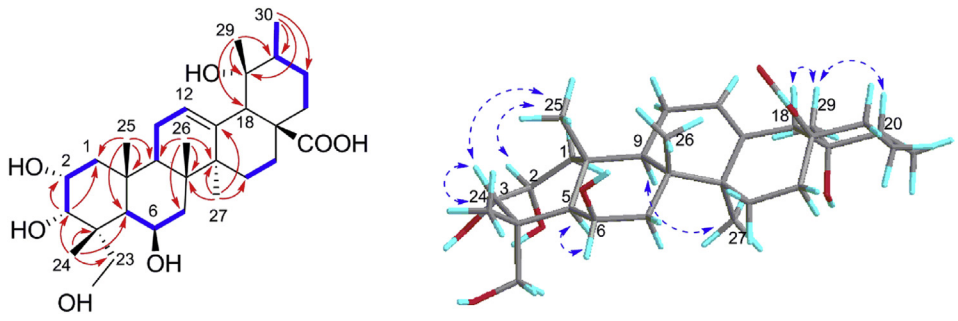

Fig. 3. Key ^1H–^1H COSY (——), HMBC (⌒), and NOE (⌒) correlations of **2**.

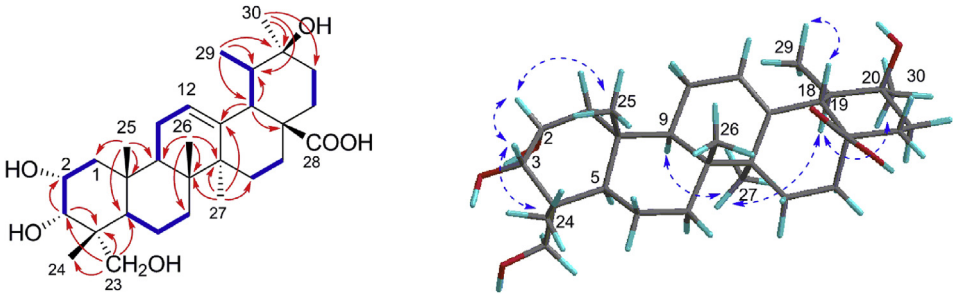

Fig. 4. Key $^{1}H-^{1}H$ COSY (—), HMBC (⌒), and ROE (⌒) correlations of **3**.

Table 2
^{1}H [ppm, mult. (*J* in Hz)] and ^{13}C NMR data of compounds **4**–**6** (in C_5D_5N).

Position	4		5		6	
	δ_C[a]	δ_H[b]	δ_C[c]	δ_H[d]	δ_C[c]	δ_H[d]
1	85.1, CH	3.72, d (9.0)	43.3, CH_2	1.94, m 1.79, m	213.5, C	–
2	74.8, CH	4.17,dd (9.0,9.0)	66.6, CH	4.28, m	45.5, CH_2	3.47,dd (12.0,12.0) 2.81,dd (12.5,5.0)
3	75.3, CH	4.32,d (9.0)	79.4, CH	4.14,d (2.0)	73.3, CH	4.58,dd (12.0,5.0)
4	43.9, C	–	42.3, C	–	44.2, C	–
5	46.0, CH	1.87, m	43.9, CH	2.04, m	47.8, CH	1.92, m
6	18.5, CH_2	1.84, m 1.61, m	18.7, CH_2	1.59, m 1.36, m	18.4, CH_2	1.77, m 1.57, m
7	33.9, CH_2	1.75, m 1.42, m	33.6, CH_2	1.71, m 1.37, m	33.1, CH_2	2.01, m 1.79, m
8	41.1, C	–	40.7, C	–	40.2, C	–
9	49.4, CH	2.17, m	48.4, CH	1.90, m	40.0, CH	2.66, m
10	43.8, C	–	38.7, C	–	52.8, C	–
11	28.0, CH_2	3.25,dt (18.0,6.0) 2.50, m	24.2, CH_2	2.08, m 2.04, m	26.2, CH_2	2.73, m 2.02, m
12	127.9, CH	5.61, br s	126.8, CH	5.44,t (3.0)	123.7, CH	5.50, br s
13	138.4, C	–	138.6, C	–	143.8, C	–
14	43.0, C	–	43.0, C	–	42.8, C	–
15	29.1, CH_2	2.33, m 1.21, m	28.9, CH_2	2.42, m 1.17, m	28.6, CH_2	2.25, m 1.11, m
16	25.4, CH_2	2.30, m 2.08, m	25.0, CH_2	2.22, m 2.04, m	23.8, CH_2	2.02, m 1.93, m
17	48.8, C	–	48.9, C	–	47.7, C	–
18	56.1, CH	2.77,d (12.0)	55.8, CH	2.64,d (12.0)	42.4, CH	3.23, m
19	38.1, CH	2.44, m	37.9, CH	2.39, m	46.3, CH_2	1.71, m 1.20, m
20	154.3, C	–	153.6, C	–	31.2, C	–
21	33.2, CH_2	2.27, m 2.40, m	32.8, CH_2	2.29, m 2.13, m	34.5, CH_2	1.33, m 1.13, m
22	40.1, CH_2	2.05, m	39.3, CH_2	2.01, m 1.79, m	33.2, CH_2	1.57, m 1.33, m
23	66.7, CH_2	4.24,d (12.0) 3.76,d (12.0)	71.7, CH_2	3.91,d (10.0) 3.76,d (10.0)	66.4, CH_2	4.14,d (10.5) 3.73,d (10.5)
24	14.8, CH_3	1.11, s	18.1, CH_3	0.87, s	14.1, CH_3	1.19, s
25	14.4, CH_3	1.37, s	17.6, CH_3	1.05, s	16.1, CH_3	1.40, s
26	18.5, CH_3	1.17, s	18.1, CH_3	1.17, s	18.6, CH_3	1.19, s
27	24.1, CH_3	1.20, s	24.0, CH_3	1.09, s	26.3, CH_3	1.21, s
28	179.9, C	–	176.0, C	–	177.0, C	–
29	17.0, CH_3	1.11,d (6.0)	16.8, CH_3	1.04,d (7.5)	33.5, CH_3	0.89, s
30	105.4, CH_2	4.81, br s 4.76, br s	105.6, CH_2	4.73, br s 4.71, br s	24.0, CH_3	0.93, s
1′			96.2, CH	6.25,d (8.5)	96.7, CH	6.24,d (7.0)
2′			74.4, CH	4.17,dd (8.5,8.5)	74.1, CH	4.20, m
3′			79.3, CH	4.27, m	78.6, CH	4.23, m
4′			71.7, CH	4.30, m	71.3, CH	4.25, m
5′			79.6, CH	4.01,ddd (9.0,4.8,2.8)	68.1, CH_2	4.39,dd (11.5,4.0) 3.84,dd (11.0,9.0)
6′			62.8, CH_2	4.45,dd (12.0,2.6) 4.38,dd (12.0,4.6)		

[a] Measured at 75 MHz.
[b] Measured at 300 MHz.
[c] Measured at 125 MHz.
[d] Measured at 500 MHz.

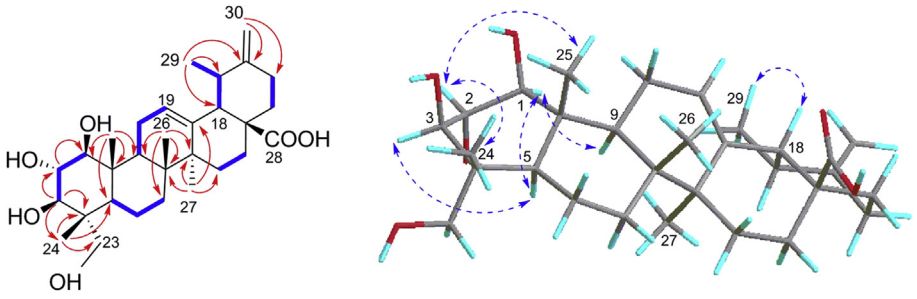

Fig. 5. Key $^{1}H-^{1}H$ COSY (—), HMBC (⌒), and NOE (⌒) correlations of **4**.

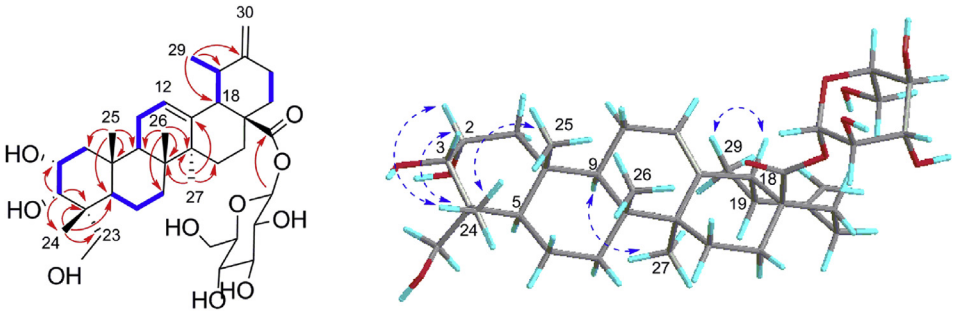

Fig. 6. Key $^{1}H-^{1}H$ COSY (—), HMBC (⌒), and NOE (⌒) correlations of **5**.

aglycone structure with 1-oxo-3β, 23-dihydroxyolean-12-en-28-oic acid 28-*O*-β-D-glucopyranoside (Yang et al., 2011). However, there was a xylopyranosyl unit instead of a β-glucopyranosyl moiety (Yoshikawa et al., 2005). The configuration of β-D-xylose was supported by the coupling constant ($J = 7.0$ Hz) and acid hydrolysis. The sugar linkage at C-28 was deduced from the HMBC correlations between H-1′(δ_H 6.24) and C-28 (δ_C 177.0) (Fig. 7). The relative configuration of **6** was also confirmed by the NOESY spectrum (Fig. 7). Thus, the structure of **6** (Fig. 1) was characterized as 1-oxo-3β, 23-dihydroxyolean-12-en-28-oic acid 28-*O*-β-D-xylopyranoside.

The five known compounds were identified as 2α,3α,23-trihydroxy-urs-12-en-28-oic acid 28-*O*-β-D-glucopyranoside (**7**) (Yang et al., 2012), 19α-hydroxyasiatic acid (**8**) (Lee et al., 2010), 2α-hydroxyursolic acid (**9**) (Cheng et al., 2010), 2*a*, 3*a*, 23-trihydroxyurs-12, 20(30)-dien-28-oic acid (**10**) (Xiao et al., 2013), and 2*a*, 3β, 23-trihydroxyurs-12, 20(30)-dien-28-oic acid (**11**) (Xiao et al., 2013) by comparison of their spectroscopic data with those reported in the literature.

All isolated compounds (**1**–**11**) were assayed for their antioxidant effects on FFA-induced hepatic steatosis in HepG2 cells. Firstly, the compounds were tested for cytotoxic activity against HepG2 cells. As shown in Fig. 8, compounds **1**–**8** and **10**–**11** had no observable effect on cell viabilities at the concentration of 10 μM, while compound **9** exhibited no cytotoxicity at 1 μM concentration. The bioassay results showed that the SOD activity were significantly decreased ($p < 0.01$) and the MDA levels were significantly increased ($p < 0.01$) when cells were incubated with FFA mixture compared with the blank group (Fig. 9). Interestingly, compounds **4**–**7** (5 μM) and **9** (1 μM) markedly increased SOD activity and reduced levels of MDA in FFA-induced HepG2 steatosis cells compared with the model group. Especially, compound **9** (1 μM) exhibited better potential effect on the inhibition of MDA production than the positive control (Vitamin E). These results implied that compounds **4**–**7** and **9** might block the development of NAFLD via ameliorating hepatic oxidative stress. However, compounds **1**–**3**, **8**, and **10**–**11** showed unfavourable effects on the antioxidant activity at the concentration of 10 μM.

Further analysis of their structures and bioactivities revealed that **1** and **4** shared the same chemical skeleton only differing in the C-30 functional group. However, their different activity suggested that the terminal double bond may be crucial for the antioxidant activity. Interestingly, compounds **10** and **11** with the terminal double bonds had no antioxidant activity, indicating that 1-hydroxy

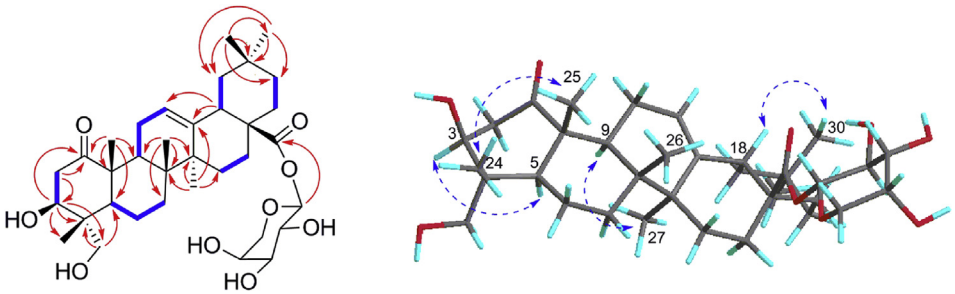

Fig. 7. Key $^{1}H-^{1}H$ COSY (—), HMBC (⌒), and NOE (⌒) correlations of **6**.

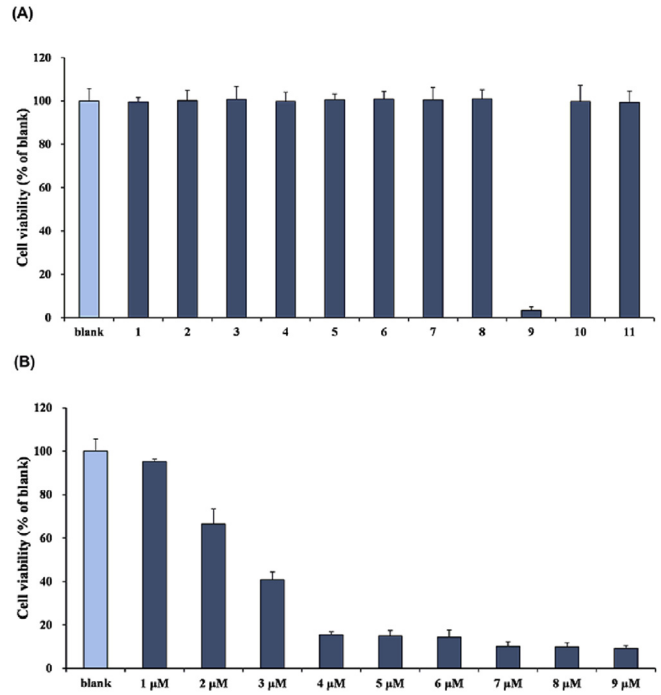

Fig. 8. The cell viability assay of compounds **1**–**11** by the MTT method. (A) Cytotoxicity of compounds **1**–**11** (10 μM). (B) Cytotoxicity of compound **9** (1–9 μM).

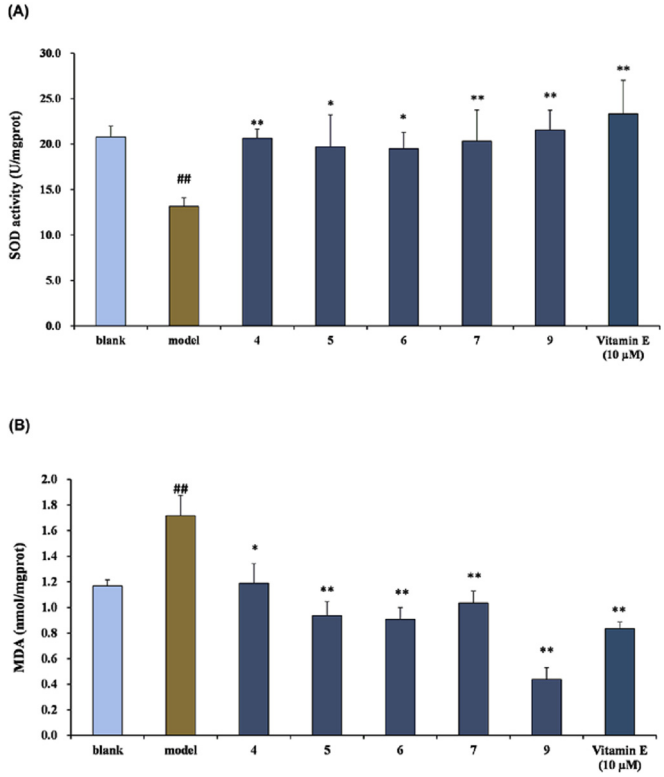

Fig. 9. Effect of compounds **4**–**7** (5 μM) and **9** (1 μM) on the levels of SOD activity (A) and MDA (B). The results include data from three experiments (mean ± SD, n = 5). $^{\#}p < 0.05$, $^{\#\#}p < 0.01$ vs blank group; $^{*}p < 0.05$, $^{**}p < 0.01$ vs model group, Student's t-test.

group may have impact on their antioxidant activities. At a concentration of 5 μM, compound **5** with pyranose showed stronger antioxidant activity than **10** without pyranose. It was proposed that the glycosyl moiety had a significant contribution to the antioxidant activity.

3. Conclusion

Phytochemical study of the leaves of *C. paliurus* generated six undescribed pentacyclic triterpenoids (**1**–**6**) and five known triterpenoids (**7**–**11**). All isolated compounds were assayed for their antioxidant effects on Free Fatty Acid-induced hepatic steatosis in HepG2 cells. Among them, three undescribed and two known triterpenoids significantly increased superoxide dismutase activity and reduced malondialdehyde level. Our findings enriched the diversity of pentacyclic triterpenoids for the genus *Cyclocarya*, and suggested that pentacyclic triterpenoids may be major functional constituents in *C. paliurus* contributing to ameliorate hepatic oxidative stress.

4. Experimental section

4.1. General experimental procedures

Optical rotations were measured in methanol using a Jasco P-1020 polarimeter. A Shimadzu UV-2500PC spectrophotometer and Nicolet Impact 410 spectrophotometer were used for recording the UV spectra (Methanol) and IR spectra (KBr pellets), respectively. 1D and 2D NMR spectra were recorded on a Bruker Avance-300 (Bruker, Switzerland, 300 MHz for ^{1}H NMR, 75 MHz for ^{13}C NMR), Bruker Avance-500 (Bruker, Switzerland, 500 MHz for ^{1}H NMR, 125 MHz for ^{13}C NMR) and Bruker Avance-600 (Bruker, Switzerland, 600 MHz for ^{1}H NMR, 150 MHz for ^{13}C NMR) NMR spectrometer with TMS as internal standard. Unless otherwise specified, chemical shifts (δ) were expressed in ppm with reference to the solvent signals, and coupling constants are expressed in hertz. HRESIMS were performed on a HP-1100 LC/EST and Synapt™ Q-TOF mass spectrometer (Waters, Milford, America). Agilent 1260 Infinity equipped with UV and Alltech 3300 ELSD detector was used to analyze the samples, and Alliance semi preparative HPLC with COSMOSIL Phecda C18 (250 mm × 20 mm, 5 μm) was applied for further purification. Column chromatography was performed with silica gel (100–200 and 200–300 mesh, Qing-dao Marine Chemical Group Co., Shandong, CN), ODS RP-18 gel (40–63 mm, Merck, Darmstadt, Germany), Sephadex LH-20 (Pharmacia, Uppsala, Sweden). D-Glucose, D-xylose, pyridine (Reagent Plus, ≥ 99%), L-cysteine methyl ester hydrochloride, and isothiocyanate were purchased from Sigma (St. Louis, MO, America). Methanol and acetonitrile (HPLC-grade) was purchased from TEDIA. All other chemicals are of analytical grade. The fractions were monitored by TLC and 1% vanillin in H_2SO_4 was used as the spraying reagent to visualize spots.

4.2. Plant material

The leaves of *C. paliurus* were collected from Nanjing Forestry University, Nanjing, Jiangsu, People's Republic of China (GPS coordinates: 118.822414, 32.085054), in October 2010 and authenticated by Prof. Minjian Qin, China Pharmaceutical University, People's Republic of China. A voucher herbarium specimen (No. L20100033) has been deposited in the herbarium of the Department of Natural Medicinal Chemistry, China Pharmaceutical University, Nanjing, Jiangsu, People's Republic of China.

4.3. Extraction and isolation

Air-dried leaves of *C. paliurus* (48.5 kg) were extracted three

times with 80% ethanol under reflux and evaporated to afford a crude extract (8.3 kg). The extract was suspended in water and partitioned with chloroform to yield a chloroform-soluble extract (3.6 kg). The chloroform extract (460 g) was subjected to a reduced pressure chromatography and eluted with gradient mixtures of CH_3Cl–MeOH (100:0, 100:3, 100:5, 5:1 and 0:100) to yield five fractions (Fr.1–5).

The isolation and purification of Fr.2 and Fr.3 have been finished in our earlier research (Wu et al., 2017).

Fr.4 (137.6 g) was chromatographed over a silica gel column and eluted with gradient mixtures of CH_3Cl–MeOH (35:1, 25:1, 15:1, 10:1, 1:1, 0:100) to obtain six subfractions (Fr.4a - 4f). Fr.4b was subjected to a Sephadex LH-20 column eluted with CH_3Cl–MeOH (1:1) to yield two subfractions (Fr.4b1 - Fr.4b2). Fr.4b1 was fractionated by silica gel column and eluted with CH_3Cl–MeOH (30:1 → 1:1) to yield four subfractions (Fr.4b1a - Fr.4b1d). Fr.4b1a was purified by semi-preparative HPLC (MeOH–H_2O, 85:15) to give **1** (25 mg), **3** (9 mg), and **9** (20 mg). Fr.4b1b was purified by semi-preparative HPLC (MeOH–H_2O, 65:25) to obtain **2** (10 mg) and **8** (35 mg). Fr.4b1c was purified by semi-preparative HPLC (MeCN–H_2O, 72:28) to yield **4** (10 mg), **10** (11 mg) and **11** (13 mg). Fr.4b2 was separated on ODS column chromatography with MeOH–H_2O (50:50 → 100:0) and purified by semi-preparative HPLC (MeCN –H_2O, 65:35) to afford **5** (8 mg), **6** (10 mg) and **7** (7 mg).

4.3.1. 1β,2a,3β,23-tetrahydroxyurs-12-en-28-ursolic acid (**1**)

White amorphous powder; $[\alpha]_D^{20}$ + 26 (*c* 0.097, MeOH); UV (MeOH) λ_{max} (log ε) 210 (2.74) nm; IR (KBr) ν_{max} 3441, 2946, 1639, 1050 cm^{-1}; ^1H and ^{13}C NMR data, see Table 1; HRESIMS *m/z* 527.3338 $[M+Na]^+$ (calcd for $C_{30}H_{48}NaO_6$, 527.3343).

4.3.2. 2a,3a,6β,19α,23-pentahydroxyurs-12-en-28-ursolic acid (**2**)

White amorphous powder; $[\alpha]_D^{20}$ + 10 (*c* 0.110, MeOH); UV (MeOH) λ_{max} (log ε) 213 (4.06) nm; IR (KBr) ν_{max} 3449, 2926, 1686, 1040 cm^{-1}; ^1H and ^{13}C NMR data, see Table 1; HRESIMS *m/z* 538.3738 $[M + NH_4]^+$ (calcd for $C_{30}H_{52}NO_7$, 538.3738).

4.3.3. 2α, 3α, 20β, 23-tetrahydroxyurs-12-en-28-ursolic acid (**3**)

White amorphous powder; $[\alpha]_D^{20}$ + 46 (*c* 0.110, MeOH); UV (MeOH) λ_{max} (log ε) 210 (3.09) nm; IR (KBr) ν_{max} 3455, 1640, 1049 cm^{-1}; ^1H and ^{13}C NMR data, see Table 1; HRESIMS *m/z* 522.3786 $[M + NH_4]^+$ (calcd for $C_{30}H_{52}NO_6$, 522.3789).

4.3.4. 1β,2a,3β,23-tetrahydroxyurs-12,20(30)-dien-28-ursolic acid (**4**)

White amorphous powder; $[\alpha]_D^{20}$ + 104 (*c* 0.097, MeOH); UV (MeOH) λ_{max} (log ε) 214 (3.64) nm; IR (KBr) ν_{max} 3449, 1633, 1050 cm^{-1}; ^1H and ^{13}C NMR data, see Table 2; HRESIMS *m/z* 520.3629 $[M + NH_4]^+$ (calcd for $C_{30}H_{50}NO_6$, 520.3633).

4.3.5. 2a, 3a, 23-trihydroxy-12, 20(30)-dien-28-ursolic acid 28-O-β-D-glucopyranoside (**5**)

White amorphous powder; $[\alpha]_D^{20}$ + 60 (*c* 0.095, MeOH); UV (MeOH) λ_{max} (log ε) 212 (4.30) nm; IR (KBr) ν_{max} 3442, 2928, 1644, 1075 cm^{-1}; ^1H and ^{13}C NMR data, see Table 2; HRESIMS *m/z* 666.4210 $[M + NH_4]^+$ (calcd for $C_{36}H_{60}NO_{10}$, 666.4212).

4.3.6. 1-oxo-3β, 23-dihydroxyolean-12-en-28-oic acid 28-O-β-D-xylopyranoside (**6**)

White amorphous powder; $[\alpha]_D^{20}$ + 55 (*c* 0.099, MeOH); UV (MeOH) λ_{max} (log ε) 210 (3.45) nm; IR (KBr) ν_{max} 3451, 2922, 1636, 1057 cm^{-1}; ^1H and ^{13}C NMR data, see Table 2; HRESIMS *m/z* 641.3653 $[M+Na]^+$ (calcd for $C_{35}H_{54}NaO_9$, 641.3660).

4.4. Acid hydrolysis of compounds **5**–**6**

Compounds **5**–**6** (each 1 mg) were hydrolyzed in 2 M HCl under reflux in a boiling water bath for 2 h. The reaction mixture was neutralized by $AgCO_3$ and extracted with $CHCl_3$ (3 × 3 mL). The aqueous layer was concentrated and dried to obtain the monosaccharide fraction. The residue was dissolved in pyridine (1 mL) containing 2 mg of L-cysteine methyl ester hydrochloride and heated at 60 °C for 1 h. Then *o*-toryl isothiocyanate (2 mg) was added and heated at 60 °C for another 1 h. The reaction mixture was analyzed by RP-HPLC under the following conditions: column, Agilent ZORBAX SB-C18 column (250 × 4.6 mm, 5 μm); solvent, 25% CH_3CN in 50 mM H_3PO_4 for 40 min; flow rate, 0.8 mL/min; detector, UV; wavelength, 250 nm; temperature, 35 °C; injection volume, 10 μL. The identification of D-glucose (t_R 17.1 min) and D-xylose (t_R 19.8 min) present in sugar fractions of compounds **5**–**6** were confirmed by comparison with those of authentic standards (Tanaka et al., 2007).

4.5. Cell culture, measurement of antioxidant enzymes and lipid peroxide, and cell viability

Human hepatoma HepG2 cells were obtained from the American Type Culture Collection (ATCC) (Shanghai, China). The cells were cultured in DMEM supplemented with 10% fetal bovine serum penicillin (100 U/ml), streptomycin (100 μg/mL) at 37 °C in a humidified atmosphere containing 5% CO_2. To induce hepatic steatosis, FFA mixture (0.33 mM palmitate and 0.66 mM oleate) (sodium salt of oleate and palmitate, Sigma, Malaysia) was added to HepG2 cells with fatty acid free bovine serum albumin as supplement in a final concentration of 1% in the culture medium as described previously (Park et al., 2017; Wobser et al., 2009). HepG2 cells were seeded into 24-well plates with 3×10^5/well. After 24 h of FFAs exposure with or without compounds (**1**–**11**), intracellular SOD and MDA content were measured by an enzymatic kit according to the manufacturer's instructions. Vitamin E (Sigma-Aldrich, St. Louis, MO, USA) served as a positive control (Gayathri et al., 2015). The effects of compounds (**1**–**11**) on cell viability were evaluated using the MTT method (Lin et al., 2015). All values were normalized by the total protein concentration of the same sample. Measurements were performed in triplicate and are representative of three independent experiments. Data analyses were performed using the software SPSS 22.0. Data were expressed as the mean ± SD. Statistical comparisons were made between groups using a one-way ANOVA and the Student–Newman–Keuls test. A value of $p < 0.05$ was considered as significant.

Author contributions

H.M. Yang and Z.Q. Yin contributed equally.

Notes

The authors declare no competing financial interest.

Acknowledgments

This research was supported by grants from the National Natural Science Foundation of China (No. 81503316, 31270673) and the Natural Science Foundation of Jiangsu Province (No. BK20161460, BK20160926).

Appendix A. Supplementary data

Supplementary data related to this article can be found at

https://doi.org/10.1016/j.phytochem.2018.03.010.

References

Cheng, J.J., Zhang, L.J., Cheng, H.L., Chiou, C.T., Lee, I.J., Kuo, Y.H., 2010. Cytotoxic hexacyclic triterpene acids from *Euscaphis japonica*. J. Nat. Prod. 73, 1655–1658.

Choi, S.S., Diehl, A.M., 2008. Hepatic triglyceride synthesis and nonalcoholic fatty liver disease. Curr. Opin. Lipidol. 19, 295–300.

Day, C.P., James, O.F.W., 1998. Steatohepatitis: a tale of two "hits"? Gastroenterology 114, 842–845.

De Almeida, B.B., Mathias, M.G., Portari, G.V., Jordao, A.A., 2010. Chronic acetonemia alters liver oxidative balance and lipid content in rats. A model of nash? Exp. Clin. Endocrinol. Diabetes 118, 61–63.

Fu, X.X., Fang, S.Z., 2009. Secondary metabolites and its physiological function of *Cyclocarya paliurus*. J. Anhui Agric. Sci. Technol. 37, 13612–13614.

Gayathri, L., Dhivya, R., Dhanasekaran, D., Periasamy, V.S., Alshatwi, A.A., Akbarsha, M.A., 2015. Hepatotoxic effect of ochratoxin A and citrinin, alone and in combination, and protective effect of vitamin E: *In vitro* study in HepG2 cell. Food Chem. Toxicol. 83, 151–163.

Jiang, C.H., Wang, Q.Q., Wei, Y.J., Yao, N., Wu, Z.F., Ma, Y.L., Lin, Z., Zhao, M., Che, C.T., Yao, X.M., Zhang, J., Yin, Z.Q., 2015a. Cholesterol-lowering effects and potential mechanisms of different polar extracts from *Cyclocarya paliurus* leave in hyperlipidemic mice. J. Ethnopharmacol. 176, 17–26.

Jiang, Y.Z., Chen, L., Wang, H., Narisi, B., Chen, B., 2015b. Li-Gan-Shi-Liu-Ba-Wei-San improves non-alcoholic fatty liver disease through enhancing lipid oxidation and alleviating oxidation stress. J. Ethnopharmacol. 176, 499–507.

Kurihara, H., Asami, S., Shibata, H., Fukami, H., Tanaka, T., 2003. Hypolipemic effect of *Cyclocarya paliurus* (Batal.) Iljinskaja in lipid-loaded mice. Biol. Pharm. Bull. 26, 383–385.

Lee, D.Y., Jung, L., Park, J.H., Yoo, K.H., Chung, I.S., Baek, N.I., 2010. Cytotoxic triterpenoids from *Cornus kousa* fruits. Chem. Nat. Compd. 46, 142–145.

Lee, I.K., Kim, D.H., Lee, S.Y., Kim, K.R., Choi, S.U., Hong, J.K., Lee, J.H., Park, Y.H., Lee, K.R., 2008. Triterpenoic acids of *Prunella vulgaris* var. *lilacina* and their cytotoxic activities *in vitro*. Arch. Pharm. Res. 31, 1578–1583.

Lee, T.H., Juang, S.H., Hsu, F.L., Wu, C.Y., 2005. Triterpene acids from the leaves of *Planchonella duclitan* (blanco) bakhuizan. J. Chin. Chem. Soc. 52, 1275–1280.

Leonarduzzi, G., Scavazza, A., Biasi, F., Chiarpotto, E., Camandola, S., Vogl, S., Dargel, R., Poli, G., 1997. The lipid peroxidation end product 4-hydroxy-2,3-nonenal up-regulates transforming growth factor β1 expression in the macrophage lineage: a link between oxidative injury and fibrosclerosis. FASEB J. 11, 851–857.

Lin, C., Huang, F., Shen, G., Yiming, A., 2015. MicroRNA-101 regulates the viability and invasion of cervical cancer cells. Int. J. Clin. Exp. Pathol. 8, 10148–10155.

Lin, Z., Wu, Z.F., Jiang, C.H., Zhang, Q.W., Ouyang, S., Che, C.T., Zhang, J., Yin, Z.Q., 2016. The chloroform extract of *Cyclocarya paliurus* attenuates high-fat diet induced non-alcoholic hepatic steatosis in Sprague Dawley rats. Phytomedicine 23, 1475–1483.

Ma, Y.L., Jiang, C.H., Yao, N., Li, Y., Wang, Q.Q., Fang, S.Z., Shang, X.L., Zhao, M., Che, C.T., Ni, Y.C., Zhang, J., Yin, Z.Q., 2015. Antihyperlipidemic effect of *Cyclocarya paliurus* (Batal.) Iljinskaja extract and inhibition of apolipoprotein B48 overproduction in hyperlipidemic mice. J. Ethnopharmacol. 166, 286–296.

Madan, K., Bhardwaj, P., Thareja, S., Gupta, S.D., Saraya, A., 2006. Oxidant stress and antioxidant status among patients with nonalcoholic fatty liver disease (NAFLD). J. Clin. Gastroenterol. 40, 930–935.

Park, Y., Sung, J., Yang, J.W., Ham, H., Kim, Y., Jeong, H.S., Lee, J.S., 2017. Inhibitory effect of esculetin on free-fatty-acid-induced lipid accumulation in human HepG2 cells through activation of AMP-activated protein kinase. Food Sci. Biotechnol. 26, 263–269.

Sashida, Y., Ogawa, K., Mori, N., Yamanouchi, T., 1992. Triterpenoids from the fruit galls of *Actinidia polygama*. Phytochemistry 31, 2801–2804.

Singab, A.N.B., El-Gendi, O.D., Kusano, A., Kusano, G., 2000. Two new triterpenic glucosidates from *Lavandula coronipifolia* in Egypt. Nat. Med. 54, 38–41.

Tanaka, T., Nakashima, T., Ueda, T., Tomii, K., Kouno, I., 2007. Facile discrimination of aldose enantiomers by reversed-phase HPLC. Chem. Pharm. Bull. 55, 899–901.

Wang, Q.Q., Jiang, C.H., Fang, S.Z., Wang, J.H., Ji, Y., Shang, X.L., Ni, Y.C., Yin, Z.Q., Zhang, J., 2013. Antihyperglycemic, antihyperlipidemic and antioxidant effects of ethanol and aqueous extracts of *Cyclocarya paliurus* leaves in type 2 diabetic rats. J. Ethnopharmacol. 150, 1119–1127.

Wang, Z.J., Xie, J.H., Shen, M.Y., Tang, W., Wang, H., Nie, S.P., Xie, M.Y., 2016. Carboxymethylation of polysaccharide from *Cyclocarya paliurus* and their characterization and antioxidant properties evaluation. Carbohydr. Polym. 136, 988–994.

Wobser, H., Dorn, C., Weiss, T.S., Amann, T., Bollheimer, C., Buttner, R., Scholmerich, J., Hellerbrand, C., 2009. Lipid accumulation in hepatocytes induces fibrogenic activation of hepatic stellate cells. Cell Res. 19, 996–1005.

Wu, Y., Li, Y.Y., Wu, X., Gao, Z.Z., Liu, C., Zhu, M., Song, Y., Wang, D.Y., Liu, J.G., Hu, Y.L., 2014. Chemical constituents from *Cyclocarya paliurus* (batal.) iljinsk. Biochem. Syst. Ecol. 57, 216–220.

Wu, Z.F., Meng, F.C., Cao, L.J., Jiang, C.H., Zhao, M.G., Shang, X.L., Fang, S.Z., Ye, W.C., Zhang, Q.W., Zhang, J., Yin, Z.Q., 2017. Triterpenoids from *Cyclocarya paliurus* and their inhibitory effect on the secretion of apoliprotein B48 in Caco-2 cells. Phytochemistry 142, 76–84.

Xiao, S.J., He, D.H., Ding, L.S., Zhou, Y., Chen, F., 2013. Triterpenes from aerial parts of *Clematoclethra scandens* subsp. *actinidioides*. China J. Chin. Mater. Med. 38, 358–361.

Xie, M.Y., Xie, J.H., 2008. Review about the research on *Cyclocarya paliurus* (batal.) Iljinskaja. J. Food Sci. Biotechnol. 27, 113–122.

Yang, H.J., Cho, H.J., Sim, S.H., Chung, Y.K., Kim, D.D., Sung, S.H., Kim, J.W., Kim, Y.C., 2012. Cytotoxic terpenoids from *Juglans sinensis* leaves and twigs. Bioorg. Med. Chem. Lett. 22, 2079–2083.

Yang, H.J., Jeong, E.J., Kim, J.W., Sung, S.H., Kim, Y.C., 2011. Antiproliferative triterpenes from the leaves and twigs of *Juglans sinensis* on HSC-T6 cells. J. Nat. Prod. 74, 751–756.

Yopp, A.C., Choti, M.A., 2015. Non-alcoholic steatohepatitis-related hepatocellular carcinoma: a growing epidemic? Dig. Dis. 33, 642–647.

Yoshikawa, K., Inoue, M., Matsumoto, Y., Sakakibara, C., Miyataka, H., Matsumoto, H., Arihara, S., 2005. Lanostane triterpenoids and triterpene glycosides from the fruit body of *Fomitopsis pinicola* and their inhibitory activity against COX-1 and COX-2. J. Nat. Prod. 68, 69–73.